physics

IMPACT FACTOR 1.5

CITESCORE 3.0

Review

The Casimir Effect in Finite-Temperature and Gravitational Scenarios

Valdir Barbosa Bezerra, Herondy Francisco Santana Mota, Augusto P. C. M. Lima, Geová Alencar and Celio Rodrigues Muniz

Special Issue

75 Years of the Casimir Effect: Advances and Prospects

Edited by

Prof. Dr. Galina L. Klimchitskaya and Prof. Dr. Vladimir M. Mostepanenko

MDPI

https://doi.org/10.3390/physics6030065

physics

MDPI

Review

The Casimir Effect in Finite-Temperature and Gravitational Scenarios

Valdir Barbosa Bezerra [1,*], Herondy Francisco Santana Mota [1], Augusto P. C. M. Lima [2], Geová Alencar [3] and Celio Rodrigues Muniz [4]

[1] Departamento de Física, Universidade Federal da Paraíba, Caixa Postal 5008, João Pessoa 58051-900, Paraíba, Brazil; hmota@fisica.ufpb.br
[2] Instituto Federal de Educação, Ciência e Tecnologia do Piauí, Campus Corrente, Rua Projetada 06, S/n, Corrente 64980-000, Piauí, Brazil; augusto.placido@ifpi.edu.br
[3] Departamento de Física, Universidade Federal do Ceará, Caixa Postal 6030, Campus do Pici, Fortaleza 60455-760, Ceará, Brazil; geova@fisica.ufc.br
[4] Faculdade de Educação, Ciências e Letras de Iguatu, Universidade Estadual do Ceará, Iguatu 63500-000, Ceará, Brazil; celio.muniz@uece.br
* Correspondence: valdir@fisica.ufpb.br

Abstract: In this paper, we review some recent findings related to the Casimir effect. Initially, the thermal corrections to the vacuum Casimir energy density are calculated, for a quantum scalar field, whose modes propagate in the (3+1)-dimensional Euclidean spacetime, subject to a nontrivial compact boundary condition. Next, we analyze the Casimir effect induced by two parallel plates placed in a weak gravitational field background. Finally, we review the three-dimensional wormhole solutions sourced by the Casimir density and pressures associated with the quantum vacuum fluctuations of the Yang-Mills field.

Keywords: Casimir effect; finite-temperature effect; nontrivial compact boundary condition; weak gravitational field; wormhole; Yang–Mills field

Citation: Bezerra , V.B.; Mota, H.F.S.; Lima, A.P.C.M.; Alencar, G.; Muniz, C.R. The Casimir Effect in Finite-Temperature and Gravitational Scenarios. *Physics* **2024**, *6*, 1046–1071. https://doi.org/10.3390/physics6030065

Received: 11 January 2024
Revised: 8 June 2024
Accepted: 5 July 2024
Published: 13 August 2024

1. Introduction

From the classical physics point of view, the phenomenon called the Casimir effect [1] cannot find its explanation. The effect manifests itself as an attractive force between the two parallel electrically neutral ideal metallic plates at zero temperature placed at a certain distance in a vacuum, according to the original configuration. According to classical electrodynamics, there is no force in such a scenario. Thus, this phenomenon can only be understood in the context of quantum physics, and its origin is related to the oscillations of the zero-point (vacuum) energy or, equivalently, to the fluctuations of the quantum electromagnetic field as a consequence of boundary conditions imposed to the field due to the presence of the plates. This is the most basic configuration that leads to the Casimir effect. This phenomenon associated with the vacuum fluctuations of the quantum electromagnetic field was predicted by Hendrik Casimir [1] in 1948, who obtained an intriguing and remarkably simple formula for this force per unit area of the plates:

$$F = -\frac{\pi^2}{240}\frac{\hbar c}{L^4}, \tag{1}$$

where L denotes the distance between the two plates and $\hbar$ and c are the reduced Planck constant and the speed of light in vacuum, respectively. That is, the force depends on a geometrical factor, the distance between the plates, and the two fundamental constants, the former related to the quantum physics and the latter one to the relativistic consideration.

Originally, the Casimir effect was associated with the electromagnetic field and material boundaries made of a perfect conductor. Thus, taking into account that the Casimir

effect, as originally conceived, is a direct consequence of the vacuum fluctuations of physical photons, whose propagating behavior depends on the presence of boundaries as compared with the free spacetime, and assuming the predictions of the quantum field theory that boundaries, independent of their nature, if material or due to the topology, induce nonzero vacuum expectation values, it is natural to expect that similar phenomena occur for countless configurations of quantum fields with different spins subject, for example, to boundary conditions dictated by the nontrivial topology associated with flat or curved spacetime [2–5].

During seventy-five years, since the discovery of this remarkable pure quantum effect, specifically from the seventies of the twentieth century up to nowadays, the line of research along the generalization described just above, in particular, concerning the role played by the nontrivial topology of spacetime on the quantum vacuum energy in the framework of the general theory of relativity, has been extensively investigated, with the breakthrough findings. As pioneering papers about this topic, we mention firstly the one that investigates the zero-point energy of quantum fields placed in background gravitational fields with a nontrivial topology [6]. As the second point, we call a cosmological model with a nontrivial topology, namely the Einstein universe with a topology $\mathcal{R}^1 \times \mathcal{S}^2$. In this cosmological scenario, considering a conformally coupled massless scalar field, the Casimir energy density and pressure are given by [7]

$$\varepsilon_0 = \frac{\hbar c}{480\pi^2 R^4} \quad \text{and} \quad P_0 = \frac{\varepsilon_0}{3}, \tag{2}$$

respectively, where R denotes the radius of the universe.

These pioneering studies inspired investigations concerning the role of the global structure of spacetime or, in other words, the role of the nontrivial topology, on the zero-point energy of quantum fields, placed in flat or curved backgrounds. Some of these studies related to the role played by boundary conditions imposed by the nontrivial topology in locally or globally flat spacetimes are given in Refs. [5,8–21]. Concerning the presence of gravitational fields, some interesting investigations were performed [4,13,22–51].

Over these seventy-five years, since its discovery [1], the Casimir effect has been actively investigated from theoretical point of view as well as experimentally. Particularly in the last three decades, and more recently, due to the possibility of numerous applications of this physical manifestation of zero-point energy, not only in fundamental sciences but also in applied sciences. It is a multidisciplinary phenomenon that arises when any quantum field is submitted to boundary conditions caused by material bodies or associated with a nontrivial space topology. It arises in different contexts, namely, quantum electrodynamics, condensed matter physics, quantum chromodynamics, gravitation and cosmology, and nanotechnology.

This paper reviews three different scenarios in which this phenomenon manifests, confirming the multifaceted and interdisciplinary features of the Casimir effect and its importance. In order to emphasize this multifaceted character, a revision is made about three different topics. The first one is related to the thermal corrections to the Casimir energy of massive and massless scalar fields, under boundary conditions with a nontrivial topology, in flat spacetime using the zeta function formalism [52]. The second concerns the investigation on how the Casimir effect manifests itself when the plates are embedded in a weak gravitational field sourced by a certain mass [50]. The third topic addressed in this review proposes the generation of wormholes in 2+1 dimensions by the Casimir energy associated to a Yang–Mills field [53]. Therefore, there is a progression in the scenarios discussed with respect to spacetime, ranging from flat one, then a slightly curved and finally a highly curved one.

The different topics considered in this review are believed to give us a better understanding of how the structure of spacetime influences a quantum phenomenon, shedding light on the relation between quantum fields, geometry and topology.

We begin by reviewing the generalized zeta function method, in Section 2. We calculate the Casimir energy for a massless scalar field and its respective thermal correction, taking into account a nontrivial compact boundary condition. In Section 3, we review the formalism to calculate the Casimir energy in a weak static gravitational field and revisit previous results of the literature. In Section 4, we study what is termed Casimir wormholes, and, in Sections 5 and 6, the summary of the results obtained and the conclusions are presented.

2. Thermal Corrections to the Casimir Energy Density: Scalar Field Subject to a Nontrivial Compact Boundary Condition

In what follows, the generalized zeta function method is used to obtain the thermal corrections to the Casimir energy density of a scalar field, initially calculated at zero temperature, by imposing a nontrivial compact boundary condition on the field. This condition was originally called the helix boundary condition in Refs. [18,54].

The expressions for the heat kernel function and free energy density are obtained in exact and analytic forms. In these calculations, quantum scalar fields with mass and those massless are taken into account. In particular, for the massless case, the internal energy density is analyzed concerning the limits corresponding to high and low temperatures. The influence of the boundary condition is the focus of the analysis along with the contribution by the thermal corrections to the Casimir energy density of the quantum scalar fields. It is worth noticing that all calculations are performed in a flat spacetime. Therefore, all modifications to the local features of the zero-point energy are due to the boundary conditions imposed on the fields.

2.1. Generalized Zeta Function Method

Let us review in what follows the vacuum energy and its temperature corrections for a real quantum scalar field with a nontrivial compact boundary condition following studies presented in Refs. [18,54,55] at zero temperature and in Ref. [52], at finite temperature. We adopt the method of the generalized zeta function defined as [56–58]

$$\zeta_4(s) = \sum_j \lambda_j^{-s}, \tag{3}$$

where λ_j represents the eigenvalues of a four-dimensional Laplace–Beltrami operator, $\hat{A}_4$, where the subindex refers to the spacetime dimension, and j takes the values $1, 2, \ldots, \infty$.

It is worth noticing that $\zeta_4(s)$ (3) converges for $\{\mathrm{Re}(s) > 2$ and it is regular at $s = 0$, in four dimensions. It can be analytically extended to the interval $\mathrm{Re}(s) < 2$, with poles at $s = 2$ and $s = 1$. As concerns its spectrum of eigenvalues denoted by λ_j, it is not necessarily discrete [58]. The path integral formulation of quantum field theory allows us to link the zeta function (3) with the partition function, Z, thus providing a way to study the thermodynamic properties of a quantum system. This connection is made through $\hat{A}_4$ and is given by [52,56,58]

$$Z = \det\left(\frac{4}{\pi\mu^2}\hat{A}_4\right), \tag{4}$$

where the parameter μ is a constant with a dimension of mass and stands for an integration measure in the functional space, and should be suppressed by the renormalization. Note that, in the case we are considering, the operator $\hat{A}_4$ is identified as the Laplace-Beltrami operator in the four-dimensional Euclidean space. Hence, in natural units, the operator has a dimension of mass squared, what makes Equation (4) dimensionless.

Upon using the known identity $e^{-\zeta_4'(0)} = \det(\hat{A}_4)$, where the prime denotes the s-derivative, from Equation (4), one finds [52,56,58]:

$$\ln Z = \frac{1}{2}\zeta_4'(0) + \frac{1}{2}\ln\left(\frac{\pi\mu^2}{4}\right)\zeta_4(0). \tag{5}$$

From Equation (5), we conclude that the partition function (4) can be determined if the zeta function (3) and its s-derivative at $s = 0$ are known.

The trace of the operator $\hat{A}_4$ defines the heat kernel $K(\eta)$:

$$K(\eta) = \mathrm{Tr}\left[e^{-\eta \hat{A}_4}\right] = \sum_j e^{-\Omega_j \eta}, \tag{6}$$

where Ω_j is the set of eigenvalues of $\hat{A}_4$. The generalized zeta function (3) can be written in terms of Equation (6) as

$$\zeta(s) = \frac{1}{\Gamma(s)} \int_0^\infty \eta^{s-1} \mathrm{Tr}\left[e^{-\eta \hat{A}_4}\right] d\eta, \tag{7}$$

where $\Gamma(s)$ is the Gamma function.

Equation (7) corresponds to another representation of the generalized zeta function (3). Note that, in representation (7), the generalized zeta function does not depend on the spacetime coordinates. The form (7) is quite helpful to calculate the vacuum free energy when the eigenvalues of the operator $\hat{A}_4$ are known. With the zeta function in hand, we just use Equation (5) to calculate the partition function and, immediately, the vacuum-free energy.

The temperature corrections enter when a periodic boundary condition is imposed on the imaginary time, τ coordinate, of the scalar field, $\phi_j(x)$, whose solution can be written as

$$\phi_j(x) = e^{-i\omega_n \tau} \varphi_\ell(\mathbf{r}) \qquad \text{with} \qquad \omega_n^2 = \left(\frac{2\pi n}{\beta}\right)^2, \tag{8}$$

where $n = 0, \pm 1, \pm 2, \ldots$, $j = (n, \ell)$ are the quantum modes and $\beta = 1/k_\mathrm{B} T$ is the period, with k_B being the Boltzmann constant and T the temperature.

The eigenvalues are given by $\lambda_n = \omega_n^2 + \mathbf{k}^2 + m^2$, with $\mathbf{k}$ being the three-momentum and m the mass of the field. The factor $\varphi_\ell(\mathbf{r})$ is the part of the solution of the quantum scalar field $\phi_j(x)$, which depends on the spatial coordinates.

It is worth pointing out that the approach we are adopting to calculate the thermal corrections are, in general, applicable, when the spacetime is ultra static [59–62], in which case, the solution can be written according to Equation (8).

Using the solution given by Equation (8), the general expression for the zeta function (7) turns into

$$\zeta_4(s) = \frac{\beta}{\sqrt{4\pi}\Gamma(s)} \left\{ \Gamma(s - 1/2)\zeta_3(s - 1/2) + 2 \sum_{n=1}^{\infty} \int_0^\infty \eta^{s-\frac{3}{2}} e^{-\frac{(n\beta)^2}{4\eta}} \mathrm{Tr}\left[e^{-\eta \hat{A}_3}\right] d\eta \right\}, \tag{9}$$

where the operator $\hat{A}_3$ with eigenvalues $\mathbf{k}$ corresponds to the spatial part of the operator $\hat{A}_4$ and $\zeta_3(s)$ is the zeta function whose general expression is given by Equation (7).

Now, Equations (5) and (9) can be used to calculate the free energy, which is given as follows:

$$\begin{aligned} F &= -\frac{\ln Z}{\beta} \\ &= \frac{1}{2}\zeta_3(-1/2) - \frac{\bar{C}_2}{2(4\pi)^2} \ln(\mathcal{C}^2) - \frac{1}{\sqrt{4\pi}} \sum_{n=1}^{\infty} \int_0^\infty \eta^{-\frac{3}{2}} e^{-\frac{(n\beta)^2}{4\eta}} \mathrm{Tr}\left[e^{-\eta \hat{A}_3}\right] d\eta, \end{aligned} \tag{10}$$

where $\sqrt{\pi}\mathrm{e}^2\mu/8$, with e being the elementary charge.

The first two terms correspond to the vacuum energy at zero temperature, and the third one furnishes the thermal corrections. Note that the result given by Equation (10)

presents an ambiguity in the definition of the vacuum energy at zero temperature if the coefficient $\bar{C}_2$ is different from zero. Let us write $\bar{C}_2$ as [4]

$$\bar{C}_2 = C_2 - C_1 m^2 + \frac{C_0 m^4}{2}, \tag{11}$$

where C_0, C_1, and C_2 are the heat kernel coefficients. It is worth calling attention to the feature that, in the massless case, the ambiguity disappears when C_2 vanishes.

The heat kernel coefficients are introduced using the heat kernel expansion [4]:

$$K(\eta) = \frac{e^{-m^2\eta}}{(4\pi\eta)^{3/2}} \sum_{p=0}^{\infty} C_{p/2}\eta^{p/2} + \mathrm{ES}, \tag{12}$$

where $C_{p/2}$ are the heat kernel coefficients and "ES" stands for exponentially suppressed terms.

To proceed with the regularization of the vacuum energy, we can write the first two terms of Equation (10) as [4]

$$E_0(s) = \frac{\mathcal{C}^{2s}}{2}\zeta_3(s - 1/2). \tag{13}$$

Therefore, the renormalized vacuum energy reads

$$E_0^{\mathrm{ren}} = \lim_{s\to 0}[E_0(s) - E_0^{\mathrm{div}}(s)], \tag{14}$$

where $E_0^{\mathrm{div}}(s)$ is the divergent contribution of the regularized expression in Equation (13) [4]. This divergent contribution is given in terms of the heat kernel coefficients $C_{p/2}$. As shown in Section 2.2 below, the only divergent contribution is given in terms of C_0, which is related to the Euclidean heat kernel divergent contribution to the zeta function $\zeta_3(s - 1/2)$. In the massive case, other coefficients appear, and thus, it is necessary to include an additional normalization condition to obtain the renormalized vacuum energy, and thus justifying the subtraction of terms proportional to the positive powers of the mass m [4]. Then, the normalization condition is given by

$$\lim_{m\to\infty} E_0^{\mathrm{ren}} = 0, \tag{15}$$

which is satisfied in the case under consideration, as expected. The condition (15) has been suggested in Ref. [63] and provides a unique physical meaning for the renormalized vacuum energy, since, in the large (infinite) mass limit, there should be no quantum vacuum fluctuations. The condition (15) implies that it is necessary to implement a renormalization of finite terms proportional to the positive powers of mass, in addition to the renormalization of infinite terms which, in general, takes place in vacuum energy configurations.

2.2. Nontrivial Compact Boundary Condition, Heat Kernel, and Thermal Corrections

In what follows, we assume that the quantum modes of the scalar field propagate in a (3+1)-dimensional Euclidean spacetime and experience a boundary condition given by

$$\varphi(x + a, y, z) = \varphi(x, y + h, z), \tag{16}$$

which is also known as the helix boundary condition in the literature [18,54]. According to Refs. [18,54], the condition (16) is topologically equivalent to a helix and the geometric parameters h and a are the pitch and the helix radius, respectively. The boundary condition expressed by Equation (16) was also considered by investigating the Casimir effect at zero [18,54] and nonzero [52] temperatures. The helix-like topology of the spacetime codified in Equation (16) is constructed using the mathematical notion of the equivalence relation, equivalence classes, and quotient space as discussed in Refs. [18,54]

(see also Ref. [64]). For instance, the points (x, y) and $(x + n_x a, y + n_y a)$ in $\mathbb{R}^2$, with $n_x, n_y = 0, \pm 1, \pm 2, \pm 3, \ldots$, present an equivalence relation if $x \to x + n_x a$ and $y \to y + n_y h$. A quotient space may be obtained by separately identifying the endpoints in each dimension x and y to form a compact space with topology $S^1 \times S^1$. Thus, we end up with two independently compactified dimensions. However, in the present case, a quotient space $\mathbb{R}^2/\backsim$ is obtained by identifying the points $(a, 0)$ and $(0, h)$, for instance, and consequently, making the direction along the green solid line in Figure 1 compact, with length $d = \sqrt{a^2 + h^2}$. Hence, the nontrivial compact condition described in Equation (16) is presented as $\mathbb{R}^2 \times \mathbb{R}^2/\backsim$.

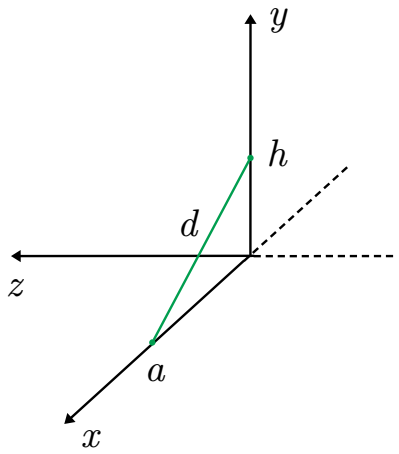

Figure 1. Illustration of the direction of the compactification. According to the condition given by Equation (16), the scalar field has the same value at $(a, 0)$ and $(0, h)$ if one considers $(x, y) = (0, 0)$. The parameters a and h can be topologically associated with a helix [18,54].

In the present study, we are interested in reviewing some important aspects of the problem related to heat kernel coefficient contributions and also to divergences associated with these coefficients.

The corresponding eigenvalues of the problem are written as [52]

$$\begin{aligned} \lambda_\ell &= k_x^2 + \left(\frac{k_x a}{h} - \frac{2\pi n}{h}\right)^2 + k_z^2 + m^2 \\ &= \left(\frac{k_y h}{a} + \frac{2\pi n}{a}\right)^2 + k_y^2 + k_z^2 + m^2. \end{aligned} \tag{17}$$

As the components of the momentum k_x and k_y are related, the spatial quantum modes are indexed by $\ell = (n, k_y, k_z)$ or $\ell = (n, k_x, k_z)$. In the calculation that follows, the latter option is assumed. Taking into account the recently obtained result concerning the heat kernel for the problem under consideration [52]:

$$K(\eta) = V \frac{e^{-m^2\eta}}{(4\pi\eta)^{3/2}} \sum_{n=-\infty}^{\infty} e^{-\frac{n^2 d^2}{4\eta}}, \tag{18}$$

where the Euclidean contribution to the heat kernel is given by [60–62]

$$K_{\mathrm{E}}(\eta) = V \frac{1}{(4\pi\eta)^{3/2}} e^{-m^2\eta}, \tag{19}$$

where only the term $n = 0$ was taken into account. Note that the heat kernel (18) can be interpreted as the one obtained from space with topology $\mathbb{R}^2 \times S^1$, with d being the size of

the compact dimension. This becomes clear if, in the first line of Equation (17), we perform the substitution

$$k_x = \frac{h}{d}\left(k_X + \frac{2a\pi n}{hd}\right), \tag{20}$$

where k_X is the momentum in the new direction, X. Hence, Equation (17) can be written as

$$\lambda_\ell \;\; = \;\; k_X^2 + \frac{4\pi^2 n^2}{d^2} + k_z^2 + m^2. \tag{21}$$

The problem considered here is equivalent to the one in a four-dimensional spacetime with Cartesian coordinates (t, X, Y, z), with the Y dimension compactified into a circle of length d [65]. In other words, the spacetime topology characterized by the condition (16) is effectively equivalent to a space with topology $\mathbb{R}^2 \times S^1$, as previously noted. That is why we have also called Equation (16) a nontrivial compact boundary condition.

Comparing the heat kernel (18) with the heat kernel expansion (18), we find that the C_0 is only coefficient different from zero and given by $C_0 = V$, where V is the volume of the (3+1)-dimensional Euclidean spacetime. It is worth calling attention to the feature that C_0 is responsible for the divergent contribution to the zeta function (7) and, thus, should be cancelled to obtain a finite result for the Casimir energy density. On the other hand, the contribution of the third term of the free energy (10), which arises from the Euclidean heat kernel (19), corresponds to the scalar thermal (blackbody) radiation contribution [56]. To find a renormalized result for the thermal correction contributions [39,40], the appropriate subtractions have to be performed. As a result, the classical limit for the free energy is recovered for high temperatures, as expected.

Now, substracting the Euclidean heat kernel contribution equation (19) from the heat kernel (18) and assuming the boundary condition given by Equation (16), the renormalized heat kernel for the field $\varphi_\ell(\mathbf{r})$ reads as :

$$K_{\rm ren}(\eta) = V\frac{e^{-m^2\eta}}{4(\pi\eta)^{3/2}}\sum_{n=1}^{\infty} e^{-\frac{n^2(a^2+h^2)}{4\eta}}. \tag{22}$$

Let us return to the generalized zeta function (7), which can be written as

$$\zeta_3(s-1/2) = V\frac{2^{3-s}m^{4-2s}}{(4\pi)^{3/2}\Gamma(s-1/2)}\sum_{n=1}^{\infty} f_{2-s}(mnd). \tag{23}$$

where

$$f_\mu(x) = \frac{K_\mu(x)}{x^\mu}, \tag{24}$$

with $K_\mu(x)$ being the modified Bessel function of the second kind.

Let us consider the free energy (10), where the first two terms correspond to the Casimir energy at zero temperature. Thus, using Equations (13) and (14), the following expression is obtained:

$$E_0^{\rm ren} = -V\frac{m^4}{2\pi^2}\sum_{n=1}^{\infty} f_2(mnd). \tag{25}$$

The result given by Equation (25) is the renormalized Casimir energy at zero temperature [18,54,55]. Taking into account the massless field, the renormalized Casimir energy can be obtained from Equation (25) assuming that the arguments of the modified Bessel function are very small, such that $K_\mu(x) \simeq (2/x)^\mu\Gamma(\mu)/2$ [66,67]. Thus, the following result is obtained [18,54,55]:

$$E_0^{\rm ren} = -V\frac{\pi^2}{90d^4}, \tag{26}$$

where the Riemann zeta function, $\zeta_{\rm R}(4) = \pi^4/90$, was used [58,66,67].

Notice that the results obtained do not depend on the energy scale, M, and as a consequence, there is no ambiguity. One should remember that the term containing the parameter M in Equation (10), which introduces an ambiguity in the definition of the vacuum energy at zero temperature, is nonzero only when the coefficient $\bar{C}_2$ in Equation (11) exists. As in the the case considered here, where $\bar{C}_2 = C_0 m^4/2$, with $C_0 = V$, as already stated in this Section. Actually, the second term on the right-hand side of Equation (10) is nonzero. However, as we expect a decreasing in the vacuum energy for large masses, this term should be discarded, since it grows with the mass m and must be subtracted in order to obey the normalization (15). Such a process, in the massive case, leads to the renormalized vacuum energy in Equation (25). On the other hand, the massless vacuum energy case does not carry the term depending on M in Equation (10) since $\bar{C}_2 = 0$. So, naturally, one obtains Equation (26).

As discussed above, the results for the Casimir energies given by Equations (25) and (26) can be obtained, effectively, by considering a space with topology $\mathbb{R}^2 \times S^1$, where one of the dimensions has been compactified into a circle of length d. But, then, what are the new features here? To answer this question, one should remember that the length d is defined in terms of the radius a and pitch h of the helix in Figure 1, i.e., $d = \sqrt{a^2 + h^2}$. This makes it possible to calculate the Casimir force both along h and a, as shwon in Ref. [18]. In Ref. [18], it is also shown that the Casimir force in the h direction behaves according to Hooke's law in the regime when the parameter ratio, $r = h/a$, is exceptionally small, i.e., $r \ll 1$, whereas in the opposite regime, $r \gg 1$, the Casimir force behaves according to an inverse square law. The helix-like topology also allows us to apply the results presented here to investigate the influence of the Casimir energy in an RNA structure of a virus like SARS-CoV-2, as has been performed in a simplified initial study in Ref. [68].

In what follows, the thermal corrections to the renormalized Casimir energy densities given by Equations (25) and (26), for the massive and massless cases, respectively, will be calculated. To do this end, the following results will be considered:

$$F_T^{\mathrm{E}} = -V \frac{m^4}{2\pi^2} \sum_{n=1}^{\infty} f_2(mn\beta), \tag{27}$$

and

$$F_T^{\mathrm{E}} = -V \frac{\pi^2}{90} (k_B T)^4 \tag{28}$$

for the massive and massless cases, respectively. Equations (27) and (28) are obtained using the Euclidean heat kernel (19). Equation (28) corresponds to the massless scalar thermal (blackbody) radiation contribution [56]. It should be subtracted from the temperature correction to obtain the classical limit at high temperatures [39,40].

The normalized temperature correction, F_T^{ren} (25), to the Casimir energy density is obtained with the use of the renormalized heat kernel equation (22).

Then, we arrives at

$$F_T^{\mathrm{ren}} = -V \frac{m^4}{\pi^2} \sum_{j=1}^{\infty} \sum_{n=1}^{\infty} f_2\Big[m\beta(j^2 + n^2\gamma^2)^{1/2}\Big], \tag{29}$$

where $\gamma = d/\beta = k_B T d$. It is worth calling attention to the feature that the result (29) is exponentially suppressed at low temperatures, which means that $\beta m \gg 1$, in which case, $K_\mu(x) \simeq \sqrt{\frac{\pi}{2x}} e^{-x}$ [66,67]. Thus, the result expressed by Equation (29) is consistent with the requirement that the temperature corrections must vanish for low temperatures. For high temperatures, which means $\beta m \ll 1$, we obtain:

$$F_T^{\mathrm{ren}} = -V \frac{2}{\pi^2} \sum_{n=1}^{\infty} \sum_{j=1}^{\infty} \frac{1}{(j^2\beta^2 + n^2 d^2)^2}. \tag{30}$$

Taking into account the massive case, the renormalized free energy is given by

$$F_T^{\text{ren}} = -V\frac{m^4}{2\pi^2}\sum_{n=1}^{\infty} f_2(mnd) - V\frac{m^4}{\pi^2}\sum_{j=1}^{\infty}\sum_{n=1}^{\infty} f_2\left[m\beta(j^2+n^2\gamma^2)^{\frac{1}{2}}\right], \tag{31}$$

where the sum of Equations (25) and (29) was considered. Note that the second term in Equation (31) is exponentially suppressed, and only the first term contributes [18,54,55].

In the massless case, Equations (26) and (30) can be combined and written as

$$F^{\text{ren}} = -V\frac{\pi^2}{90d^4} - V\frac{2}{\pi^2}\sum_{n=1}^{\infty}\sum_{j=1}^{\infty}\frac{1}{(j^2\beta^2+n^2d^2)^2}. \tag{32}$$

In this case, the low and high temperatures limit can be analyzed and interesting results are obtained. Firstly, let us perform the sum in j in Equation (32), to obtain the high-temperature limit. In what concerns the limit of low temperatures, it is obtained by performing the sum in n, firstly. Taking these procedures into account, the result obtained for the high-temperature limit, $k_BTd \gg 1$, is as follows:

$$F_{\text{ren}} \simeq -\frac{k_BT}{2\pi d^3}\zeta_3 - \frac{2(k_BT)^2}{d^2}e^{-2\pi\gamma}. \tag{33}$$

Note that the second term in Equation (33) is exponentially suppressed, while the first one corresponds to the classical scenario and dominates in this limit.

In the low-temperature limit, Equation (32) turns into

$$F_{\text{ren}} \simeq -\frac{\pi^2}{90d^4} + \frac{\pi^2}{90}(k_BT)^4 - \frac{(k_BT)^3}{2\pi d}\zeta(3) - \frac{2(k_BT)^3}{\pi d}e^{-\frac{2\pi}{k_BTd}}. \tag{34}$$

Note that the first term corresponds to the Casimir energy at zero temperature and is the dominant one. In what concerns to the third term, it is exponentially suppressed.

3. Casimir Energy in Weak Static Gravitational Field

When comprehensively examining the Casimir Effect in curved spacetime, special consideration should be given to scenarios involving weak background gravity. This assertion stems from the anticipation that feasible laboratory conditions for assessing the interaction between vacuum energy and gravity will likely involve relatively small gravitational effects. For instance, the Archimedes experiment [69,70] aims to measure the weight of the vacuum and is expected to occur in such a setting. The initial results of this experiment are eagerly awaited, as they may offer a means to scrutinize the reality of the vacuum fluctuation energy and its gravitational behavior further. From a theoretical standpoint, researchers generally expect the vacuum energy to behave following the principle of equivalence, a fundamental aspect of general relativity. However, experimental confirmation is still pending.

In this Section, we review the fundamentals of the Casimir effect in curved spacetime and revisit several works from the literature that delve into the simplest case of a Casimir apparatus subjected to weak, spherically symmetrical gravity, a suitable approximation for Earth's gravitational field. We begin with an elegant and explicit calculation introduced by Francesco Sorge in Ref. [44], along with similar findings from other sources. Subsequently, we discuss the corrections proposed by Augusto Lima and colleagues in Ref. [50], leading to a somewhat surprising prediction of null corrections to the measured "vacuum weight" at the first relevant order. This contradicts some earlier works that suggest that the Casimir energy should be affected by gravity like any other form of energy. We then briefly outline how Sorge resolves this issue in Ref. [71].

3.1. General Method

Firstly, let us review the method for computing the Casimir effect in curved spacetime highlighting a simplified approach proposed in Ref. [44]. This involves studying the Casimir effect in the basic scenario of rectangular parallel plates under Dirichlet boundary

conditions, considering a real massless scalar field within a static weak gravitational field. The configuration is shown in Figure 2.

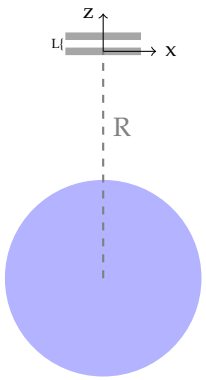

Figure 2. Diagram illustrating the placement of plates and the observer's coordinate system.

In a curved spacetime, the action of the scalar field, ϕ, can be written as

$$S = \int \mathrm{d}^4x\sqrt{g}\left[\frac{1}{2}g^{\mu\nu}\partial_\mu\phi\partial_\nu\phi + \frac{1}{2}\epsilon\mathcal{R}\phi^2\right], \tag{35}$$

and the field equation as

$$\frac{1}{\sqrt{g}}\partial_\mu[\sqrt{g}g^{\mu\nu}\partial_\nu\phi] + \epsilon\mathcal{R}\phi = 0, \tag{36}$$

where $g^{\mu\nu}$ is the 4-dimensional metric tensor with a signature (+,−,−,−), the Greek indices take the values 0 (temporal component), 1, 2, and 3 (spatial components), g is the determinant of $g^{\mu\nu}$, ϵ denotes the vacuum energy, $\mathcal{R}$ is the Ricci scalar, and $\partial_\mu \equiv \partial/\partial x_\mu$.

In order to get a simple enough expression for the energy density, we consider a static observer who performs measurements with the four-velocity:

$$u^\mu = g_{00}^{-1/2}\delta_0^\mu, \tag{37}$$

where δ_ν^μ is the Kronecker delta.

The orthonormal mode solutions obey the scalar product:

$$\langle\phi_n, \phi_m\rangle = \int_\Sigma \sqrt{g_\Sigma}n^\mu[\phi_n^*\partial_\mu\phi_m - (\partial_\mu\phi_n^*)\phi_m]d\Sigma, \tag{38}$$

where Σ stands for the boundaries, and

$$\langle(\phi_n, \vec{k}_n), (\phi_m, \vec{k}_m)\rangle = \delta(\vec{k}_n - \vec{k}_m)\delta_{nm}, \tag{39}$$

with n and m representing discrete modes, while $\vec{k}$ refers to the transverse wave numbers, and $\delta(\vec{k}_n - \vec{k}_m)$ is the Dirac delta function.

The mean vacuum energy is defined as

$$\bar{\epsilon} = \frac{1}{V_p}\int_\Sigma d^3x\sqrt{g_\Sigma}u^\mu u^\nu\langle 0|T_{\mu\nu}|0\rangle, \tag{40}$$

where V_p is the proper volume of the cavity $V_p = \int_\Sigma d^3x\sqrt{g_\Sigma}$ and $T_{\mu\nu}$ represents the stress–momentum–energy of the scalar field. In terms of the field modes, Equation (40) can be written in terms of the orthonormal mode solutions as [44]

$$\bar{\epsilon} = \frac{1}{V_p}\sum_n\int d^2k\sqrt{g_\Sigma}(g_{00})^{-1}T_{00}[\phi_n^*, \phi_n], \tag{41}$$

where, $T_{00}[\phi_n^*, \phi_n]$ represents a bilinear form analogous to the time–time component of the stress–energy tensor:

$$T_{00}[\phi_n^*, \phi_n] = \partial_0\phi_n^*\partial_0\phi_n - g_{00}g^{\mu\nu}\partial_\mu\phi_n^*\partial_\nu\phi_n. \tag{42}$$

3.2. Sorge's Result and Generalizations

The field is governed by the ordinary Klein–Gordon equation; the boundaries are planes with coordinate separation, L; and field obeys the conditions $\phi(z = 0) = \phi(z = L) = 0$. The orthonormal solutions are given by

$$\phi(x) = \frac{1}{2\pi\sqrt{\omega_{nF}L}}\sin\Big(\frac{n\pi z}{L}\Big)\exp[i(\omega_{nF}t - k_\perp x_\perp)], \tag{43}$$

where $\omega_{nF} = \sqrt{k_\perp^2 + (n\pi/L)^2}$ is the mode frequency (with the $\perp$ subscript denoting the transverse component and the "F" subscript standing for a flat spacetime). Using these mode solutions in Equations (41) and (42), we obtain:

$$\bar{\epsilon} = \frac{1}{8\pi^2 L}\sum_n \int \mathrm{d}^2k_\perp \omega_{nF}. \tag{44}$$

Employing Schwinger's proper time representation and zeta function regularization, we arrive at the renormalized value for the Casimir energy in Minkowski spacetime:

$$\bar{\epsilon}_{\mathrm{Cas}} = -\frac{\pi^2}{1440L^4}. \tag{45}$$

To explore the curved case, we commence with the explicit calculation proposed by Sorge [44]. The spacetime metric is defined as

$$ds^2 = -(1 + 2\Phi(r))dt^2 + (1 - 2\Phi(r)(dr^2 + r^2d\Omega^2)), \tag{46}$$

where r is the radius-vector, Ω is the space solid angle, $\Phi(r) = -\mathcal{M}/r$ is the Newtonian gravitational potential, with $\mathcal{M}$ being the mass parameter, in the framework of the weak field approximation of the Schwarzschild spacetime. In this background, the Casimir energy is sought in a scenario where two parallel rectangular plates are present. To simplify the calculations, a Cartesian-like coordinate system is employed between the plates, whose origin is located at the center of the lower plate, and the z-axis is aligned parallel with the radial direction (see Figure 2).

Concerning the metric, it is written as

$$ds^2 = -(1 + 2\Phi_0 + 2\mathrm{Y}z)dt^2 + (1 - 2\Phi_0 - 2\mathrm{Y}z)(dx^2 + dy^2 + dz^2). \tag{47}$$

Applying the following coordinate changes: $dt \to (1 + 2\Phi_0)^{-1}dt$, $\vec{dx} \to (1 - 2\Phi_0)^{-1}\vec{dx}$, the metric (47) turns into

$$ds^2 = -(1 + 2\mathrm{Y}z)dt^2 + (1 - 2\mathrm{Y}z)\vec{dx}^2, \tag{48}$$

which reduces to Equation (47) with $\Phi_0 = 0$. Therefore, up to order $(\mathcal{M}/R)^2$, the relevant parameter is Y. Notice that, in the case where there are no crossing terms in the metric, the Casimir energy for a general constant perturbation measured by the observer, given by Equation (37), remains unaltered [72]. This is what is expected because this spacetime is equivalent to the Minkowski one.

The vacuum expected value of the energy–momentum tensor can then be determined by the standard manner using orthonormal solutions of the Klein–Gordon Equation (36) and substituting into Equation (41).

The perturbative calculation is performed, order by order [44], starting with the zeroth order (flat spacetime) and, in the sequel, to the first order (up to Φ_0 in Equation (47)). An intriguing observation is that, when calculating to the order of Φ_0—constant perturbative terms relative to Minkowski spacetime—it is demonstrated that there is no correction to the conventional flat spacetime Casimir energy. This stems from the observation that setting $\mathrm{Y} = 0$ in Equation (47) results in a flat spacetime with a gauge transformation [44]. Then, we proceed to the second-order calculation following these steps.

The case $\mathrm{Y} = 0$ corresponds to the first-order approximation being calculated explicitly, with a null result [44]. In the sequel, the correction of the second order of the metric (48) is taken into account. In this case, the field equation turns into

$$-(1 - 4\mathrm{Y}z)\partial_t^2\phi + \nabla^2\phi = 0, \tag{49}$$

where $\nabla^2 \equiv \delta^{ij}\partial_i\partial_j$. The solutions are, then, given by

$$\phi_{n,k} = \chi_n(z)e^{i\omega_n t - ik_\perp x_\perp}, \tag{50}$$

and asymptotically turn into

$$\chi_n(u) = A_n u^{-1/4}\sin\left(\frac{2}{3}u^{3/2} + \varphi\right), \tag{51}$$

where

$$u(z) = -(z - p/q)q^{1/3},\ q = 4\mathrm{Y}\omega_n^2,\ p = \omega_n^2 - k_\perp^2, \tag{52}$$

and $\omega_n = (1 + \mathrm{Y}L)\omega_{nF}$ are the frequencies. In the results obtained in Ref. [44], the expansion is performed in terms of the solution for the flat case, as follows:

$$\phi_n = \phi_n^{(0)} + \delta\phi_n. \tag{53}$$

Using this approach, the energy–momentum tensor and Casimir energy can be written as

$$T_{00}[\phi_n^*, \phi_n] = T_{00}[\phi_n^{(0)*}, \phi_n^{(0)}] + \{T_{00}[\delta\phi_n^*, \phi_n^{(0)}] + \mathrm{c.c}\}, \tag{54}$$

and $\bar{\epsilon} = \bar{\epsilon}^{(0)} + \delta\bar{\epsilon}$. Here, "c.c." stands for complex conjugate.

Substituting the first term on the right-hand side of Equation (54) into Equation (41) and subsequently renormalizing, we obtain:

$$\bar{\epsilon}_{\mathrm{ren}}^{(0)} = -(1 - 2\mathrm{Y}L_p)\frac{\pi^2}{1440L_p^4}. \tag{55}$$

In the expression (55), $L_p = \int dz\sqrt{|g_{33}|}$ represents the proper separation distance between the plates.

Considering the second term, which is analogous to the flat spacetime expression (44), the calculation is performed by integrating the frequency change of the modes (neglecting other terms since $\delta\phi$ itself is of order Y):

$$\delta\bar{\epsilon} = \frac{1}{8\pi^2 L}\sum_n \int d^2k_\perp \delta\omega_n = \mathrm{Y}L_p\left(-\frac{\pi^2}{1440L_p^4}\right), \tag{56}$$

with the following result:

$$\bar{\epsilon}_{\mathrm{Cas}} = -(1 - \mathrm{Y}L_p)\frac{\pi^2}{1440L_p^4} = -(1 - \mathrm{Y}L)\bar{\epsilon}_0, \tag{57}$$

with $\bar{\epsilon}_0$ being the standard flat spacetime result. Notably, in Ref. [44] it is meticulously ensured that the result is expressed exclusively in terms of proper quantities, not in the coordinate ones. This constitutes the original outcome presented in Ref. [44].

Several generalizations to the result (57) have been proposed, such as one in Ref. [73] where a general weak field metric is suggested by considering distincts Φ and Υ parameters as follows:

$$ds^2 = -(1 + 2\Phi_0 + 2\Upsilon_0 z)dt^2 + (1 - 2\Phi_1 - 2\Upsilon_1 z)(dx^2 + dy^2 + dz^2). \tag{58}$$

Taking into account the Neumann boundary conditions, a calculation can be carried out for both scalar and vector fields. In particular, for a real scalar massless field, the following result for the proper energy density is obtained:

$$\bar{\epsilon} = -(1 + \Phi_0 + \Upsilon_0 \frac{L_p}{2})\bar{\epsilon}_0. \tag{59}$$

This approach can be applied to specific cases, including the far-field limit of Kerr spacetime (also discussed in Ref. [74]), Fermi spacetime, and the scenario of Horava–Lifshitz gravity with a cosmological constant. This can be achieved by adjusting the coefficients Φ and Υ. It is important to note however, that Equation (59) does not seem to recover the result obtained in Equation (57). Several additional examples involving spacetimes sharing some similarity with Equation (58) are explored. These include the study of a similar model for extended theories of gravity [75], the Casimir effect in post-Newtonian gravity with Lorentz violation [76], and the Casimir effect in quadratic theories of gravity [77].

3.3. Revisiting

Recently, Lima and colleagues [50] have revisited the the problem we consider here addressed by Sorge in Ref. [44]. Let us first revisit Sorge's approach [44] to calculate second-order corrections. The same reasoning that leads to the second-order calculations can be applied to compute the first-order correction; let us examine the outcome.

Assuming that $\Phi = \Phi_0$ in Equation (46) and substituting Equation (45) into Equation (42) and integrating, we obtain

$$\bar{\epsilon}^0 = \frac{1}{V_p}\frac{1}{(2\pi)^2 2L}(1 - 3\Phi_0)\sum_n \int d^2k\omega_0. \tag{60}$$

Performing the renormalization and writing the result in terms of L_P, we find

$$\bar{\epsilon}^0_{\text{ren}} = -(1 - 4\Phi_0)\frac{\pi^2}{1440L_p^4}. \tag{61}$$

The frequencies are $\omega \simeq (1 + 2\Phi_0)\omega_0$, so we should have

$$\delta\bar{\epsilon} = -2\Phi_0\frac{\pi^2}{1440L_p^4}. \tag{62}$$

Adding the contributions given in Equations (61) and (62), a nonzero energy shift is found. The method falters due to the assumption that $\delta\bar{\epsilon}$ can be computed by substituting ω_0 for $\delta\omega$, as in the flat spacetime case.

Lima and colleagues [50] demonstrated that this is not the case and that the correction factor is linked to a geometrical term reminiscent of the normalization condition (38). In what follows, the details are presented.

Let us begin by writing Equation (51) as a perturbative expansion in terms of Υ, as follows

$$\chi(z) = \frac{1}{2\pi\sqrt{\omega_0 L}}\sin\left(\frac{n\pi z}{L}\right) + \Upsilon\chi^{(1)}(z) + \mathcal{O}(\mathcal{M}/R)^3, \tag{63}$$

where $\chi^{(1)}$ defines the first order correction. To obtain $\chi^{(1)}$, we have to determine A_n, φ and ω_n. The frequencies are obtained by imposing the periodicity of the solution, namely, $\phi(0) = \phi(L) = 0$, which gives us

$$\omega_n \simeq (1 + \mathrm{Y}L)\omega_0, \quad \text{where} \quad \omega_0 = [k^2 + (n\pi/L)^2]^{1/2}. \tag{64}$$

Imposing that $\chi(z = 0) = 0$, the following solution is obtained:

$$\phi = -\frac{2}{3}u^{3/2}(0). \tag{65}$$

To obtain the coefficients A_n, let us write Equation (38) by restricting to the hypersurface $t = 0$. Thus, the following normalization condition is obtained:

$$\langle \chi(n, k_1), \chi(n, k_2) \rangle = \delta^2(k_{1\perp} - k_{2\perp})\delta_{nm}, \tag{66}$$

and as a consequence,

$$A_n = \left[(2\pi)^2 2\omega \int_V d^3x(1 - 4\mathrm{Y}z))\Theta_n^2] \right]^{-1/2} \text{ with } \Theta_n = u^{-1/4} \sin\left(\frac{2}{3}u^{3/2} + \varphi\right). \tag{67}$$

Now, let us use the results for A_n, φ and ω_n in the expansion of Equation (51) in powers of Y, similarly to Equation (63). As a result, we get

$$\chi^{(1)}(z) = [2n\pi\omega_0^2 L^2(L - z)z\cos(n\pi z/L) + L(2n^2\pi^2 z + 2k^2L^2z - k^2L^3)\sin(n\pi z/L)]/4Ln^2\pi^3\sqrt{\omega_0 L}. \tag{68}$$

The solution given by Equation (63), can be used to verify that the Klein–Gordon equation given by Equation (36), along with the boundary condition and normalization relation, is satisfied up to order $(M/R)^2$.

Now, we have all the necessary information to write Equation (41). In order to do this, let us express Equation (42) in terms of $\chi(z)$, as

$$T_{00}[\psi_n^*, \psi_n] = \frac{1}{2}\omega_n^2\chi_n^2 + \frac{1}{2}(1 + 4\mathrm{Y}z)[k_\perp^2\chi_n^2 + (\partial_z\chi_n)^2]. \tag{69}$$

Thus, the unnormalized vacuum energy density reads

$$\bar{\epsilon} = \frac{1}{V_p}\frac{S}{8\pi^2 L}(1 + \mathrm{Y}L/2)\sum_n \int d^2k_\perp \omega_0, \tag{70}$$

while the renormalized Casimir energy density is given by

$$\bar{\epsilon}_{\mathrm{Cas}} = -\frac{\pi^2}{1440L^4}(1 + 2\mathrm{Y}L) = -\frac{\pi^2}{1440L_p^4} = \bar{\epsilon}_0. \tag{71}$$

Therefore, regarding the proper length of the cavity, measured by a static observer, the mean value of the Casimir energy density is identical to the one obtained in a flat spacetime case, for a rigid cavity.

Verify if the result (71) has important consequences is challenging. As it is written in generalized coordinates, this verification should be not straightforward.

To distinguish between physical effects and those arising due to the choice of coordinates. The Casimir energy density appears to be the same as that obtained in the case of flat spacetime, where there is no imposition of boundary onditions, for instance. Setting aside

these considerations from a heuristic perspective, it is intriguing that the shift in the field solution found in this calculation is sufficient to compensate for the geometrical factors.

Furthermore, in Ref. [50], it is demonstrated that the above conclusion also holds for the case of the more general metric (58). According to the this new result (71), there would be no correction to the Casimir energy and, consequently, no correction to the force between the plates, in the presence of weak field gravity. The initial calculation seems to yield a seemingly controversial result, which might not align with the equivalence principle.

The question of whether or not the vacuum should gravitate by the principle of equivalence has been explored in earlier papers [78–81]. These papers are dedicated to the question "How does Casimir energy fall?" and conduct in-depth analyses with a seemingly general agreement that the buoyancy of the vacuum energy should indeed obey the equivalence principle. Following this line of reasoning, we conclude that, although the calculations following from the definition given by Equation (40) have been performed correctly, the obtained result, given by Equation (71), is not consistent with the equivalence principle, since to obey this principle in the order of approximation considered, a term of Newtonian potential energy would be expected, highly suggesting there is a problem with the initial proposition.

Returning to the earlier discussion, presented in Section 3.2, a new calculation for the Casimir energy in the presence of weak gravity was conducted in Ref. [31], this time and using the Schwinger method [82,83], the same result given by Equation (57) was obtained. With respect to the results expressed by Equation (71), it was also obtained in Ref. [84].

Going deeper, in Ref. [71], Sorge proposes another method of obtaining the vacuum energy by calculating the quasi-local Tolman mass of the vacuum between the plates. Additional insight is provided for the meaning (or lack thereof) of expression (41), which represents a summation of the expectation value for the energy–momentum tensor taken in the frame of a series of different observers. Since a single observer cannot simultaneously measure values for the entire region with infinite points, this does not reflect a measurable experimental result.

Through a detailed formal calculation, the Sorge demonstrates that the total measured energy for the system at a specific instant in time should be

$$E_t = \int_\Sigma d^3x \sqrt{|g|} \langle T^0{}_0 \rangle_{\text{vac}}. \tag{72}$$

When compared to the density definition (41), it becomes apparent that the former is missing an extra $\sqrt{|g_{00}|}$ factor, attributed to a redshift factor between the local observer and an ideal one at spatial infinity.

It is then demonstrated through a Lagrangian method that the energy attributed to the Casimir apparatus subjected to a weak gravitational field at a given time t, in the laboratory frame of a Fermi observer, is

$$E = -\left[1 + \Upsilon\left(H + \frac{L_p}{2}\right)\right] S_p \frac{\pi^2}{1400 L_p^3} = \left[1 + \Upsilon\left(H + \frac{L_p}{2}\right)\right] V_p \bar{\epsilon}_0, \tag{73}$$

where H is the reference height of the lower plate in the laboratory frame. This implies that the correction,

$$\delta E = \Upsilon\left(H + \frac{L_p}{2}\right) V_p \bar{\epsilon}_0, \tag{74}$$

acts as a gravitational potential energy, where $z_{\text{cm}} \equiv H + L_p/2$ is the vertical coordinate of the center of mass of the vacuum field, being then in concordance with the principle of equivalence. Notice that this result is in accordance with the one obtained in Ref. [73] if one takes $H \to R$. Nazari also proposes a quasi-local stress–tensor formalism in Ref. [85], although the results differ from those obtained by Sorge [31].

As it is stressed by Sorge and Nazari, for typical values of the Y factor on Earth's surface, corrections proposed to the Casimir energy due to the planet's gravitational field are quite small (approximately 10^{-22}-times the value of the ordinary Casimir interaction), but the possibilities of measuring these effects have been discussed since Ref. [43]. Those discussions may be of help to fuel the idealization of the Archimedes experiment [69,70].

In Ref. [86], an instructive analysis is carried out for the problem of a rigid Casimir cavity radially falling in geodesic motion towards a Schwarzschild event horizon. In this case, on the comoving observer frame, the horizon gives rise to a non-static background. It is found that, still in a perturbative approach (although it is outlined that the method proposed could be a starting point to a nonperturbative one), through the effective action method, somewhat small corrections to the proper energy density related to vacuum polarization (static Casimir effect) and the creation of quanta inside the cavity. It is shown that the energy variations considering both aspects coincide precisely, suggesting the two contributions might be intrinsically related, although, as already pointed out this is quite complicated to ensure because of the perturbative first-order nature of the calculations carried out.

In Ref. [87], several earlier results are generalized in the analysis of a Casimir apparatus orbiting in a background described by the Kerr spacetime. In paper [87], rather than calculating the effects due to the variation of the geometry inside the cavity, the metric components are taken as approximately constant inside the plates, and instead, lower order (bigger magnitude) corrections due to the nonstatic nature of spacetime are obtained, related to the loss of azimuthal symmetry in this scenario. Some limiting cases are considered such as those when the orbit is close to a null path, and thus, the measured energy approaches zero; this case is also close to the case of the innermost stable circular orbits of extremal Kerr black holes, as pointed out in Ref. [87]. Another noticeable result of Ref. [87] is that observers with zero angular momentum relative to the source will detect no disturbance in the ordinary Casimir interaction.

References [86,87] exemplify even more relevant subjects such as tidal and dynamic effects on the vacuum state, which may be found considering time-dependent backgrounds and stronger gravitational effects. Further details of the Casimir effect in gravitational spacetimes such as Kerr and Schwarzschild ones are forseeing to be uncovered in the forthcoming years, although more detailed calculations involving variations of the energy–momentum tensor in small Casimir cavities involving factors such as plate finiteness and anisotropies in the field solutions may prove to be cumbersome. Likewise, one may also expect many exciting results to arise from the study of vacuum energy in the context of other feature-rich objects, such as wormholes.

Different extensions of the elementary particles Standard Model predict the existence of light massive and massless elementary particles [88,89], which can be exchanged between atoms of material bodies separated by a given distance implying the appearance of corrections to Newton's gravitational law of the Yukawa-type as well as the power type [90]. The deviation from Newtonian gravity is commonly investigated by fixing the constraints on the parameters of non-Newtonian gravity performed using the experiments of Eötvos and Cavendish types [90]. One limitation of this kind of experiments is that the strength of the obtained constraints quickly decreases when the bodies are separated by distances below a few micrometers. At such distances, the Casimir force [1] becomes dominant as compared to Newton's gravitational force. In this case, the investigations concerning non-Newtonian interactions are of crucial importance as may reveal some insight into how to connect the two apparently incompatible theoretical pillars of modern physics, namely quantum mechanics and general relativity. This makes the search for non-Newtonian gravity at considerably short separations an important scientific problem to be considered, and, in addition, the measurements of the Casimir force appear as important data that can be used to obtain stronger constraints on the parameters that measure the deviations from Newtonian gravity, due to hypothetical interactions predicted in different unification schemes beyond the Standard Model. During the last two decades, measurements of the Casimir interaction

were performed using different configurations [91–99], and, as a consequence, there was a significant improvement concerning the constraints on the Yukawa-type corrections to Newton's gravitational law. The present generation of experiments to measure the Casimir force permits us to impose strong constraints on chameleon cosmological models [100]. Concerning the symmetrons [101], some results were addressed recently [102], even in a scenario of a hypothetical Casimir experiment. As was shown above, to explain the deviations from Newton's law of gravitation at sub-millimeter separations between macroscopic bodies, the measure of the Casimir force with high accuracy has a fundamental role, not only concerning the comprehension of this specific point, but also to clarify on the questions related to the dark sector and a new physics phenomenology. To improve the acquisition of data related to this measurements. The Casimir And Non-Newtonian force EXperiment (CANNEX) is a project to allow for the measurements of the force between parallel macroscopic plates separated by distances between 3 and 30 micrometers [103,104]. The improvement of the apparatus sensitivity, with the CANNEX, may potentially open a window to detect several physical phenomena beyond the Standard Model and general relativity based on the quantum phenomenon termed the Casimir effect.

4. Casimir Wormholes

The distinctive feature of the Casimir energy density lies in its ability to violate energy conditions, notably attaining negative values for specific configurations. This unique property turns the Casimir energy density a rare energy source with the potential to facilitate the existence of traversable wormholes, as discussed in Ref. [105]. These objects are solutions to Einstein's equations, akin to hypothetical spacetime tunnels connecting distant points in the universe. Traversable wormholes typically necessitate the presence of exotic matter, as outlined in Ref. [106]. However, it is worth noting that certain modified theories of gravity, as explored in Ref. [107], have offered alternative perspectives on this requirement, which has proven to be instrumental in the study of such exotic structures [108,109].

The pioneering exploration of the energy–momentum tensor associated with the Casimir effect as a potential contributor to the building of four-dimensional traversable wormholes within the framework of general relativity emerged in 2019 through the research of Remo Garattini [110]. Garattini's study [110] resulted in the derivation of the following "Casimir" wormhole solution, characterized by a throat radius denoted as r_0. In the form of a Morris–Thorne solution, one has:

$$ds^2 = -e^{2\Phi(r)}dt^2 + \frac{dr^2}{1 - b(r)/r} + r^2 d\Omega^2, \tag{75}$$

with the shape function $b(r)$ given by

$$b(r) = \frac{2r_0}{3} + \frac{r_0^2}{3r}, \tag{76}$$

and the redshift function $\Phi(r)$ is

$$\Phi(r) = \log\left(\frac{3r}{3r + r_0}\right). \tag{77}$$

It is worth calling attention to the feature that such a solution obeys the traversability conditions that should be satisfied by a wormhole, namely:

(i) the flaring-out condition, determined by the minimality of the wormhole throat, which imposes that $(b - b'r)/b^2 > 0$, where the "prime" means derivative with respect to r and at the throat, $b(r_0) = r_0$;
(ii) the condition to guarantee the existence of wormholes, given by $1 - b/r \geq 0$; and finally,

(iii) the condition that there are no horizons, which are identified by the existence of surfaces with $e^{\Phi} \to 0$, so that $\Phi(r)$ is finite everywhere [106].

It is worth mentioning that the solution given by Equations (75)–(77) adheres to the Casimir equation of state (EoS), $p_r = 3\rho = -3\pi^2/(720r^4)$, where the radial coordinate replaces the customary separation between plates, hence the denomination "Casimir wormholes". A criticism that can be made to this direct approach is that, to build a complete wormhole solution using quantum fields, one must simultaneously solve the quantum field theory and the gravitational equations, thus accounting for the backreaction of the renormalized stress–energy tensor of the quantum fields beyond the linearized (or perturbative) approximation.

Soon after, the Garattini study [110] was followed by various others in the same line of investigation, including modified theories [111–118], and expanded to encompass d spacetime dimensions, as documented in Ref. [119]. Nonetheless, the research of Geová Alencar, Valdir Bezerra and Celio Muniz [120] has revealed that, within the context of 2+1 dimensions, the Casimir energy density and pressure alone do not have the necessary attributes to support a wormhole structure. Consequently, it is not feasible to create what may be referred to as "pure" Casimir wormholes within this reduced dimension, as elaborated upon in Ref. [120].

Three-Dimensional Casimir–Yang–Mills Wormholes

Motivated by earlier investigations that explored the utilization of quarkonic matter as a catalyst for wormholes, as referenced in Ref. [121], the pursuit of discovering traversable Casimir wormholes confined to 2+1 dimensions has been revisited. This re-evaluation was prompted by adopting a perspective based on the Casimir effect of gluon fields, as expounded upon in Ref. [53]. This new approach involves considering the potentials derived from lattice simulations based on first principles within the Yang–Mills theory, characterizing the interactions between perfect chromoelectric conductors at both short and long distances, as initially presented in Ref. [122]. In Ref. [122], the lattice calculation of the Casimir energy for the SU(N) gauge theory was fitted by the following expression:

$$\frac{\mathcal{E}}{L} = -\mathrm{Dim}G\frac{\zeta(3)}{16\pi}\frac{\left(R\sqrt{\sigma}\right)^{-\nu}}{R^2}e^{-M_{\mathrm{Cas}}R}, \tag{78}$$

where Dim$G$ is the dimension of the group (Dim(SU(3)) = 3; for the group SU(3), L is the length of each wire, R is the distance between them, and σ is the tension of the confining (fundamental) Yang–Mills string at zero temperature). The exponent ν represents an anomalous dimension of the Casimir potential at short distances and M_{Cas} represents the effective Casimir mass associated with the nonperturbative mass gap at large distances. The quantities ν and M_{Cas} are free parameters that can be controlled to obtain the best lattice fit. It is worth mentioning that the Casimir energy of the non-interacting case (short distances) is obtained by performing $\nu = M_{\mathrm{Cas}} = 0$ in the expression (78) above.

With this motivation, an innovative approach has been introduced in the quest for a traversable Casimir wormhole solution within lower dimensions in the context of the vacuum fluctuations of Yang–Mills fields. This approach entails introducing a subtle perturbation to the EoS, which relates Casimir energy density to the corresponding pressure, by incorporating a series of functions characterized by inverse power laws relative to the radial coordinate. This perturbation was taken into account in both the short- and long-range interactions of the referenced quantum fields, as comprehensively detailed in Ref. [53], yielding distinct classes of static and circularly symmetric Casimir wormhole solutions. By averaging such deformation in the EoS, the authors identified that the original equation of state is maintained, and therefore, it forms a legitimate Casimir source on average. The energy conditions and stability of these novel solutions were studied in detail.

In this context of three-dimensional Casimir–Yang–Mills wormholes, we focus on the long-range interaction case, where a Casimir mass, denoted as $M_{\rm Cas}$, is associated with gluons. The simplest wormhole solution within the obtained spectrum of solutions can succinctly be described as follows. In terms of the shape function, we have [53]:

$$b(r) = r_0 + 2\kappa\lambda\sigma^{-\frac{\nu}{2}} M_{\rm Cas}^{\nu+1} r[\Gamma(-\nu-1, M_{\rm Cas} r) - \Gamma(-\nu-1, M_{\rm Cas} r_0)], \tag{79}$$

where $\Gamma(a, z)$ is the incomplete gamma function. For the redshift function, we obtain

$$\Phi(r) = \frac{r_0}{2r}(2+\nu+M_{\rm Cas} r_0) + \frac{1}{2} M_{\rm Cas} r_0 \ln\left(\frac{r}{r_0}\right) - \frac{r_0(\nu - M_{\rm Cas} r_0)}{r - r_0} \ln\left(\frac{r}{r_0}\right). \tag{80}$$

The metric functions (79) and (80) ensure the asymptotic local flatness and flaring-out conditions of the wormhole solution. It is interesting to note the nontrivial topology that emerges from this solution, since asymptotically, it presents a conical singularity behavior, i.e.,

$$\frac{b(r)}{r} \approx -2\kappa\lambda\sigma^{-\frac{\nu}{2}} M_{\rm Cas}\Gamma(-\nu-1, M_{\rm Cas} r_0), \tag{81}$$

which does not happen in the short-distance scenario.

Another interesting aspect of the analysis involves the examination of the solution stability through the adiabatic sound velocity, v_s, within the source, v_s, defined as

$$v_s^2(r) = \frac{1}{2}\left[\frac{d(p_r + p_\theta)}{d\rho}\right] = \frac{1}{2}\left[\frac{p_r'(r) + p_\theta'(r)}{\rho'(r)}\right]. \tag{82}$$

In the expression (82), p_r and p_θ represent the radial and lateral pressures, respectively. It is worth noting that, in contrast to the short-range case, only the long-range interaction case exhibits stability ($v_s \geq 0$), and the sound velocity remains less than 1 nearby and on the wormhole throat, lending physical significance to this solution as can be seen in the parameter space depicted in Figure 3.

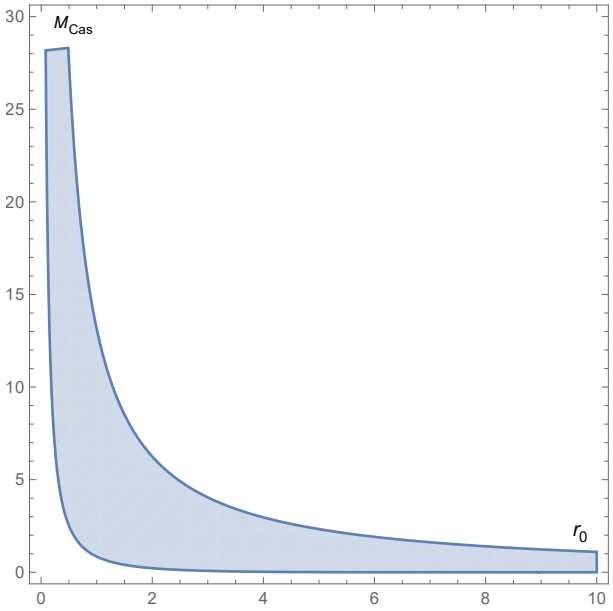

Figure 3. Parameter space $(r_0, M_{\rm Cas})$ nearby the Casimir–Yang–Mills wormhole throat ($r \approx r_0$) for the simplest solution of the interacting scenario, pointing out the region in which $0 \leq v_s^2 \leq 1$, with $\nu = 0.05$, $\lambda = 3\zeta(3)/(16\pi)$. See text for details.

Energy conditions also were evaluated, and as anticipated, violations were indeed observed. This finding is in line with the expectations, since it is consistent with the negative Casimir energy density serving as the primary source for these wormhole solutions.

5. Summary of Results

The generalized zeta function method and the heat kernel expansion were used to obtain the renormalized free energy for massive and massless scalar fields, at zero temperature, as well as the thermal corrections, in a closed and analytic form. These studies were performed in Minkowski spacetime, by imposing on the fields a nontrivial compact boundary condition. In the massless case, the limits of high and low temperatures were obtained and discussed.

A discussion was presented about the explicit derivation of the Casimir interaction from quantum field orthonormal solutions. It emphasizes the problem related to the energy definition in the equation and its implications, in particular the conclusion of the absence of sensible corrections to the Casimir force due to gravity. This is a reminder that energy, as a non-local quantity, presents difficulty with its definition in curved spacetime. It was shown that this problem is solved with more thorough treatment involving the quasi-local formalism, and the results were reconciled with the principle of equivalence.

Finally, a traversable wormhole solution was obtained by considering the Casimir energy associated with the quantum vacuum fluctuations of the Yang–Mills field in a three-dimensional spacetime, as a source of the gravitating body.

Quantum fields, as exemplified in this study, are confined to a bounded domain with nontrivial compact boundary conditions. These fields experience influences due to the bounded nature of the space and the imposed boundary conditions. Additionally, when a finite temperature is considered, it also impacts the Casimir effect, as expected.

Concerning the Casimir energy of a scalar field placed in a weak gravitational field, between two parallel plates, the obtained result tells us that this energy depends exclusively on the proper values of the quantities involved in the energy expression.

Finally, the wormhole solution sourced by a Casimir energy of Yang–Mills origin was considered. It was shown that the energy conditions are violated, as expected. Another point analyzed concerns the stability of the solution, which is present only in the long-range interaction regime. In this regime, an asymptotic conical singularity also occurs.

6. Conclusions and Discussion

Let us summarize the findings of this study.

First, we have obtained the Casimir energy density with thermal corrections for a quantum scalar field, with and without mass, in a (3+1)-dimensional Euclidean spacetime, under the restriction that the field obeys a nontrivial compact boundary condition. To find this result, we used the generalized zeta function method and the renormalized heat kernel expansion given by Equation (22), which can be written as the sum of the $n = 0$ term, corresponding to the Euclidean contribution, given by Equation (19). When using the Euclidean heat kernel to obtain the free energy at zero temperature, we faced a problem, namely the appearance of a divergence term. This problem is solved by appropriately subtracting this divergence. Concerning the thermal corrections, in the massive case, the Euclidean heat kernel gives a finite contribution, while for the massless case, a blackbody radiation contribution is obtained, as shown in Equation (27)). Even being finite, these contributions should also be subtracted, to obtain the correct classical limit at high temperature, for the massless scalar field. The renormalization approach used to calculate the vacuum energy at zero temperature and nonzero temperatures gives us exact and analytic results for the renormalized free energy (31) and (32) for both cases, namely massive and massless, respectively.

In the particular case of the massless field, it was shown that the free energy density (32) has asymptotic behaviors, concerning the temperature, which permits us to write down the free energy density in a relatively simple and appropriate form to analyze the high-temperature and low-temperature limits. Performing the sum concerning j, the high-temperature limit is obtained as in Equation (33), and the correct classical limit is confirmed, as one would expect. On the other hand, when the sum is firstly performed over n in Equation (32), the low-temperature limit is achieved, as shown in Equation (34).

As a final observation related to this topic on the influence of nontrivial compact boundary conditions, as well as of the finite temperature, the results obtained show explicitly the changes in the physical observables due to the nontrivial condition imposed on the quantum scalar fields, for both cases, massive and massless, as well as the changes due to the finite-temperature effect, expressed by the thermal correction.

In Section 3, in the second part of this paper, we briefly discussed the explicit derivation of the Casimir interaction from quantum field orthonormal solutions in a weak gravitational field. However, as demonstrated, an issue arises due to the energy definition in Equation (41), leading to the conclusion that meaningful corrections to the Casimir force caused by gravity are absent. This highlights the challenge of obtaining total energies, which are non-local quantities in curved spacetime. A more comprehensive treatment involving quasi-local formalism reconciles the results with the equivalence principle. Although it is predicted that vacuum energy should gravitate like any other form of energy, experimental confirmation is still pending. Therefore, the results of the Archimedes experiment are eagerly awaited as they are believed to bring breakthrough measurements.

The Casimir energy's capacity to violate energy conditions has moved researchers to explore its potential in forming traversable wormholes, which connect distant regions or universes. Garattini's paper introduced the concept of Casimir wormholes [110], but integrating quantum field theory and gravity to form complete solutions consistently is still a challenge. Studies exploring modified theories and higher dimensions have demonstrated that Casimir energy does not provide support for wormholes in 2+1 dimensions. However, as we have shown, a recent investigation into the Casimir effects associated with Yang–Mills fields ([53]) uncovered various feasible classes of three-dimensional traversable Casimir wormholes by introducing perturbations to the linear equation of state. While energy condition violations were observed, stable solutions emerged in the long-range interaction scenario hinting at potential physical validity. In addition, an asymptotic conical singularity-like behavior emerged due to the intricate interplay between the strong Yang–Mills field dynamics and the spacetime geometry. The study aimed to enhance the comprehension of the relationship between the Casimir energy and the emergence of spacetime structures including those with nontrivial topologies.

Thus, we reviewed three theoretical scenarios that have been approached in recent years. The one scenario considered was one related to thermal corrections of the Casimir effect considering the influence of helix boundary conditions dictated by the topology. In the other case, the influence of a weak gravitational field on a Casimir apparatus formed by two parallel plates placed in a vacuum with this field was considered. Finally, a three-dimensional configuration corresponding to a non-Abelian field as a source to shape a static and circularly symmetric traversable wormhole was considered where the Casimir effect is present.

There are several directions research connected with the Casimir effect. For example, those concerning the interaction between two mirrors mediated by massive fermion fields, such as quarks or neutrinos, and the effect of the topology, among many others. However, despite the intensive researches in the field over the last seventy-five years, quite a number of problems stay unsolved up to nowadays. Thus, after seventy-five years, scientists will have several mysteries to discover and applications to find, certainly, related to the Casimir effect, a pure quantum manifestation of zero-point energy.

Author Contributions: Conceptualization, H.F.S.M., C.R.M., G.A. and V.B.B.; methodology, H.F.S.M., C.R.M., G.A., A.P.C.M.L. and V.B.B.; software, H.F.S.M., C.R.M., A.P.C.M.L. and G.A.; validation, H.F.S.M., C.R.M., G.A. and V.B.B.; formal analysis, H.F.S.M., C.R.M., G.A., A.P.C.M.L. and V.B.B.; investigation, H.F.S.M., C.R.M., G.A., A.P.C.M.L. and V.B.B.; resources, H.F.S.M., C.R.M., A.P.C.M.L. and G.A.; writing—original draft preparation, H.F.S.M., C.R.M., G.A. and V.B.B.; writing—review and editing, H.F.S.M., C.R.M., G.A., A.P.C.M.L. and V.B.B.; visualization, H.F.S.M., C.R.M., G.A., A.P.C.M.L. and V.B.B.; supervision, V.B.B.; project administration, V.B.B.; funding acquisition, H.F.S.M., C.R.M., G.A. and V.B.B. All authors have read and agreed to the published version of the manuscript.

Funding: This research was funded by Conselho Nacional de Desenvolvimento Científico e Tecnológico (CNPq)-Brazil. V.B.B. is partially supported by the Conselho Nacional de Desenvolvimento Científico e Tecnológico (CNPq)-Brazil, through the Research Project No. 307211/2020-7. H.E.S.M. is partially supported by the Conselho Nacional de Desenvolvimento Científico e Tecnológico (CNPq)-Brazil, through the Research Project No. 308049/2023-3. G.A. is partially supported by the Conselho Nacional de Desenvolvimento Científico e Tecnológico (CNPq)-Brazil, through the Research Project No. 315568/2021-6. C.R.M. is partially supported by the Conselho Nacional de Desenvolvimento Científico e Tecnológico (CNPq)-Brazil, through the Research Project No. 308168/2021-6.

Data Availability Statement: No new data were created or analyzed in this study. Data sharing is not applicable to this article.

Conflicts of Interest: The authors declare no conflicts of interest.

References

1. Casimir, H.B.G. On the attraction between two perfectly conducting plates. *Proc. Kon. Nederland. Akad. Wetensch. B* **1948**, *51*, 793–795. Available online: https://dwc.knaw.nl/DL/publications/PU00018547.pdf (accessed on 1 July 2024).
2. Mostepanenko, V.M.; Trunov, N.N. *The Casimir Effect and Its Applications*; Clarendon Press/Oxford University Press Inc.: New York, NY, USA, 1997. [CrossRef]
3. Milton, K.A. *The Casimir Effect: Physical Manifestations of Zero-Point Energy*; World Scientific Ltd.: Singapore, 2001. [CrossRef]
4. Bordag, M.; Klimchitskaya, G.L.; Mohideen, U.; Mostepanenko, V.M. *Advances in the Casimir Effect*; Oxford University Press Inc.: New York, NY, USA, 2009. [CrossRef]
5. Bordag, M.; Mohideen, U.; Mostepanenko, V.M. New developments in the Casimir effect. *Phys. Rep.* **2001**, *353*, 1–205. [CrossRef]
6. DeWitt, B.S. Quantum field theory in curved space–time. *Phys. Rep.* **1975**, *19*, 295–357. [CrossRef]
7. Ford, L.H. Quantum vacuum energy in general relativity. *Phys. Rev. D* **1975**, *11*, 3370–3377. [CrossRef]
8. Müller, D.; Fagundes, H.V.; Opher, R. Casimir energy in multiply connected static hyperbolic universes. *Phys. Rev. D* **2002**, *66*, 083507. [CrossRef]
9. Ferrer, E.J.; de la Incera, V.; Romeo, A. Photon propagation in spacetime with a compactified spatial dimension. *Phys. Lett. B* **2001**, *515*, 341–347. [CrossRef]
10. Lima, M.P.; Müller, D. Casimir effect in E^3 closed spaces. *Class. Quant. Grav.* **2007**, *24*, 897–914. [CrossRef]
11. Cao, C.; van Caspel, M.; Zhitnitsky, A.R. Topological Casimir effect in Maxwell electrodynamics on a compact manifold. *Phys. Rev. D* **2013**, *87*, 105012. [CrossRef]
12. Bessa, C.H.G.; Bezerra, V.B.; Silva, J.C.J. Casimir effect in spacetimes with cosmological constant. *Int. J. Mod. Phys. D* **2016**, *25*, 1641017. [CrossRef]
13. Bezerra de Mello, E.R.; Saharian, A.A. Topological Casimir effect in compactified cosmic string spacetime. *Class. Quant. Grav.* **2012**, *29*, 035006. [CrossRef]
14. Mota, H.F.; Bezerra, V.B. Topological thermal Casimir effect for spinor and electromagnetic fields. *Phys. Rev. D* **2015**, *92*, 124039. [CrossRef]
15. Bellucci, S.; Saharian, A.A.; Saharyan, N.A. Casimir effect for scalar current densities in topologically nontrivial spaces. *Eur. Phys. J. C* **2015**, *75*, 378. [CrossRef]
16. Dowker, J.S. Spherical universe topology and the Casimir effect. *Class. Quant. Grav.* **2004**, *21*, 4247–4272. [CrossRef]
17. Asorey, M.; García-Álvarez, D.; Muñoz-Castañeda, J.M. Casimir effect and global theory of boundary conditions. *J. Phys. A Math. Gen.* **2006**, *39*, 6127–6136. [CrossRef]
18. Feng, C.-J.; Li, X.-Z. Quantum spring from the Casimir effect. *Phys. Lett. B* **2010**, *691*, 167–172. [CrossRef]
19. Bezerra, V.B.; Mota, H.F.; Muniz, C.R. Remarks on a gravitational analogue of the Casimir effect. *Int. J. Mod. Phys. D* **2016**, *25*, 1641018. [CrossRef]
20. Kleinert, H.; Zhuk, A. The Casimir effect at nonzero temperatures in a universe with topology $S^1 \times S^1 \times S^1$. *Theor. Math. Phys.* **1996**, *108*, 1236–1248. [CrossRef]
21. Tanaka, T.; Hiscock, W.A. Massive scalar field in multiply connected flat spacetimes. *Phys. Rev. D* **1995**, *52*, 4503–4511. [CrossRef] [PubMed]
22. Dowker, J.S.; Critchley, R. Covariant Casimir calculations. *J. Phys. A Math. Gen.* **1976**, *9*, 535–540. [CrossRef]

23. Ford, L.H. Quantum vacuum energy in a closed universe. *Phys. Rev. D* **1976**, *14*, 3304–3313. [CrossRef]
24. Dowker, J.S. Thermal properties of Green's functions in Rindler, de Sitter, and Schwarzschild spaces. *Phys. Rev. D* **1978**, *18*, 1856. [CrossRef]
25. Altaie, M.B.; Dowker, J.S. Spinor Fields in an Einstein universe: Finite temperature effects. *Phys. Rev. D* **1978**, *18*, 3557–3564. [CrossRef]
26. Baym, S.S.; Oezcan, M. Casimir energy in a curved background with a spherical boundary: An exactly solvable case. *Phys. Rev. D* **1993**, *48*, 2806–2812. [CrossRef]
27. Karim, M.; Bokhari, A.H.; Ahmedov, B.J. The Casimir force in the Schwarzschild metric. *Class. Quant. Grav.* **2000**, *17*, 2459–2462. [CrossRef]
28. Setare, M.R.; Mansouri, R. Casimir effect for spherical shell in de Sitter space. *Class. Quant. Grav.* **2001**, *18*, 2331–2338. [CrossRef]
29. Elizalde, E.; Nojiri, S.; Odintsov, S.D.; Ogushi, S. Casimir effect in de Sitter and anti-de Sitter brane worlds. *Phys. Rev. D* **2003**, *67*, 063515. [CrossRef]
30. Aliev, A.N. Casimir effect in the spacetime of multiple cosmic strings. *Phys. Rev. D* **1997**, *55*, 3903–3904. [CrossRef]
31. Sorge, F. Casimir effect in a weak gravitational field: Schwinger's approach. *Class. Quant. Grav.* **2019**, *36*, 235006. [CrossRef]
32. Konno, K.; Takahashi, R. Spacetime rotation-induced Landau quantization. *Phys. Rev. D* **2012**, *85*, 061502. [CrossRef]
33. Elizalde, E. Uses of zeta regularization in QFT with boundary conditions: A cosmo-topological Casimir effect. *J. Phys. A Math. Gen.* **2006**, *39*, 6299–6307. [CrossRef]
34. Bezerra de Mello, E.R.; Bezerra, V.B.; Saharian, A.A. Electromagnetic Casimir densities induced by a conducting cylindrical shell in the cosmic string spacetime. *Phys. Lett. B* **2007**, *645*, 245–254. [CrossRef]
35. Elizalde, E.; Odintsov, S.D.; Saharian, A.A. Repulsive Casimir effect from extra dimensions and Robin boundary conditions: From branes to pistons. *Phys. Rev. D* **2009**, *79*, 065023. [CrossRef]
36. Elizalde, E.; Saharian, A.A.; Vardanyan, T.A. Casimir effect for parallel plates in de Sitter spacetime. *Phys. Rev. D* **2010**, *81*, 124003. [CrossRef]
37. Nouri-Zonoz, M.; Nazari, B. Vacuum energy and the spacetime index of refraction: A new synthesis. *Phys. Rev. D* **2010**, *82*, 044047. [CrossRef]
38. Saharian, A.A.; Setare, M.R. Casimir effect for curved boundaries in Robertson–Walker spacetime. *Class. Quant. Grav.* **2010**, *27*, 225009. [CrossRef]
39. Bezerra, V.B.; Klimchitskaya, G.L.; Mostepanenko, V.M.; Romero, C. Thermal Casimir effect in closed Friedmann universe revisited. *Phys. Rev. D* **2011**, *83*, 104042. [CrossRef]
40. Bezerra, V.B.; Mostepanenko, V.M.; Mota, H.F.; Romero, C. Thermal Casimir effect for neutrino and electromagnetic fields in closed Friedmann cosmological model. *Phys. Rev. D* **2011**, *84*, 104025. [CrossRef]
41. Nazari, B.; Nouri-Zonoz, M. Electromagnetic Casimir effect and the spacetime index of refraction. *Phys. Rev. D* **2012**, *85*, 044060. [CrossRef]
42. Milton, K.; Saharian, A.A. Casimir densities for a spherical boundary in de Sitter spacetime. *Phys. Rev. D* **2012**, *85*, 064005. [CrossRef]
43. Calloni, E.; Di Fiore, L.; Esposito, G.; Milano, L.; Rosa, L. Vacuum fluctuation force on a rigid Casimir cavity in a gravitational field. *Phys. Lett. A* **2002**, *297*, 328–333. [CrossRef]
44. Sorge, F. Casimir effect in a weak gravitational field. *Class. Quant. Grav.* **2005**, *22*, 5109–5119. [CrossRef]
45. Bimonte, G.; Esposito, G.; Rosa, L. From Rindler space to the electromagnetic energy–momentum tensor of a Casimir apparatus in a weak gravitational field. *Phys. Rev. D* **2008**, *78*, 024010. [CrossRef]
46. Lin, F.L. Casimir effect of graviton and the entropy bound. *Phys. Rev. D* **2001**, *63*, 064026. [CrossRef]
47. Ruser, M.; Durrer, R. Dynamical Casimir effect for gravitons in bouncing braneworlds. *Phys. Rev. D* **2007**, *76*, 104014. [CrossRef]
48. Drut, J.E.; Porter, W.J. Convexity of the entanglement entropy of SU(2N)-symmetric fermions with attractive interactions. *Phys. Rev. Lett.* **2015**, *114*, 050402. [CrossRef] [PubMed]
49. Sorge, F. Gravitational memory of Casimir effect. *Phys. Rev. D* **2023**, *108*, 104003. [CrossRef]
50. Lima, A.P.C.M.; Alencar, G.; Muniz, C.R.; Landim, R.R. Null second order corrections to Casimir energy in weak gravitational field. *J. Cosmol. Astropart. Phys.* **2019**, *07*, 011. [CrossRef]
51. Muniz, C.R.; Bezerra, V.B.; Cunha, M.S. Casimir effect in the Hořava–Lifshitz gravity with a cosmological constant. *Annals Phys.* **2015**, *359*, 55–63. [CrossRef]
52. Aleixo, G.; Mota, H.F.S. Thermal Casimir effect for the scalar field in flat spacetime under a helix boundary condition. *Phys. Rev. D* **2021**, *104*, 045012. [CrossRef]
53. Santos, A.C.L.; Muniz, C.R.; Maluf, R.V. Yang–Mills Casimir wormholes in D = 2 + 1. *J. Cosmol. Astropart. Phys.* **2023**, *09*, 022. [CrossRef]
54. Zhai, X.-H.; Li, X.-Z.; Feng, C.-J. The Casimir force of quantum spring in the $(D+1)$-dimensional spacetime. *Mod. Phys. Lett. A* **2011**, *26*, 669–679. [CrossRef]
55. Feng, C.-J.; Li, X.-Z. Quantum spring. *Int. J. Mod. Phys. Conf. Ser.* **2012**, *7*, 165–173. [CrossRef]
56. Hawking, S.W. Zeta function regularization of path integrals in curved spacetime. *Commun. Math. Phys.* **1977**, *55*, 133–148. [CrossRef]

57. Elizalde, E. Zeta function regularization in Casimir effect calculations and J.S. Dowker's contribution. *Int. J. Mod. Phys. Conf. Ser.* **2012**, *14*, 57–72. [CrossRef]
58. Elizalde, E.; Odintsov, S.D.; Romeo, A.; Bytsenko, A.A.; Zerbini, S. *Zeta Regularization Techniques with Applications*; World Scientific Publishing: Singapore, 1994. [CrossRef]
59. Sonego, S. Ultrastatic space-times. *J. Math. Phys.* **2010**, *51*, 092502. [CrossRef]
60. Pontual, I.; Moraes, F. Casimir effect around a screw dislocation. *Philos. Mag. A* **1998**, *78*, 1073–1084. [CrossRef]
61. Cognola, G.; Kirsten, K.; Vanzo, L. Free and selfinteracting scalar fields in the presence of conical singularities. *Phys. Rev. D* **1994**, *49*, 1029–1038. [CrossRef] [PubMed]
62. Bytsenko, A.A.; Cognola, G.; Vanzo, L. Vacuum energy for (3+1)-dimensional spacetime with compact hyperbolic spatial part. *J. Math. Phys.* **1992**, *33*, 3108–3111. [CrossRef]
63. Bordag, M. Ground state energy for massive fields and renormalization. *arXiv* **1998**, arXiv:hep-th/9804103. [CrossRef]
64. Nakahara, M. *Geometry, Topology and Physics*; CRC Press/Taylor & Francis Group: Boca Raton, FL, USA, 2003. [CrossRef]
65. Farias Junior, A.J.D.; Mota Santana, H.F. Loop correction to the scalar Casimir energy density and generation of topological mass due to a helix boundary condition in a scenario with Lorentz violation. *Int. J. Mod. Phys. D* **2022**, *31*, 2250126. [CrossRef]
66. Abramowitz, M.; Stegun, I.A. (Eds.) *Handbook of Mathematical Functions with Formulas, Graphs, and Mathematical Tables*; Dover Publications, Inc.: New York, NY, USA, 1972. Available online: https://archive.org/details/handbookofmathe000abra/ (accessed on 1 July 2024).
67. Gradshteyn, I.S.; Ryzhik, I.M. *Table of Integrals, Series, and Products*; Academic Press/Elsevier Inc.: San Diego, CA, USA, 2014. [CrossRef]
68. Nogueira, B.; Lavor, I.; Muniz, C. Ribonucleic acid genome mutations induced by the Casimir effect. *Biosystems* **2023**, *226*, 104888. [CrossRef]
69. Calloni, E.; De Laurentis, M.; De Rosa, R.; Garufi, F.; Rosa, L.; Di Fiore, L.; Esposito, G.; Rovelli, C.; Ruggi, P.; Tafuri, F. Towards weighing the condensation energy to ascertain the Archimedes force of vacuum. *Phys. Rev. D* **2014**, *90*, 022002. [CrossRef]
70. Avino, S.; Calloni, E.; Caprara, S.; De Laurentis, M.; De Rosa, R.; Di Girolamo, T.; Errico, L.; Gagliardi, G.; Grilli, M.; Mangano, V.; et al. Progress in a vacuum weight search experiment. *Physics* **2020**, *2*, 1–13. [CrossRef]
71. Sorge, F. Quasi-local Casimir energy and vacuum buoyancy in a weak gravitational field. *Class. Quant. Grav.* **2020**, *38*, 025009. [CrossRef]
72. Zhang, A. Theoretical analysis of Casimir and thermal Casimir effect in stationary space–time. *Phys. Lett. B* **2017**, *773*, 125–128. [CrossRef]
73. Nazari, B. Casimir effect of two conducting parallel plates in a general weak gravitational field. *Eur. Phys. J. C* **2015**, *75*, 501. [CrossRef]
74. Bezerra, V.B.; Mota, H.F.; Muniz, C.R. Casimir effect due to a slowly rotating source in the weak field approximation. *Phys. Rev. D* **2014**, *89*, 044015. [CrossRef]
75. Lambiase, G.; Stabile, A.; Stabile, A. Casimir effect in extended theories of gravity. *Phys. Rev. D* **2017**, *95*, 084019. [CrossRef]
76. Blasone, M.; Lambiase, G.; Petruzziello, L.; Stabile, A. Casimir effect in Post-Newtonian gravity with Lorentz-violation. *Eur. Phys. J. C* **2018**, *78*, 976. [CrossRef]
77. Buoninfante, L.; Lambiase, G.; Petruzziello, L.; Stabile, A. Casimir effect in quadratic theories of gravity. *Eur. Phys. J. C* **2019**, *79*, 41. [CrossRef]
78. Fulling, S.A.; Milton, K.A.; Parashar, P.; Romeo, A.; Shajesh, K.V.; Wagner, J. How does Casimir energy fall? *Phys. Rev. D* **2007**, *76*, 025004. [CrossRef]
79. Milton, K.A.; Parashar, P.; Shajesh, K.V.; Wagner, J. How does Casimir energy fall? II. Gravitational acceleration of quantum vacuum energy. *J. Phys. A Math. Theor.* **2007**, *40*, 10935–10943. [CrossRef]
80. Shajesh, K.V.; Milton, K.A.; Parashar, P.; Wagner, J.A. How does Casimir energy fall? III. Inertial forces on vacuum energy. *J. Phys. A Math. Theor.* **2008**, *41*, 164058. [CrossRef]
81. Milton, K.A.; Shajesh, K.V.; Fulling, S.A.; Parashar, P. How does Casimir energy fall? IV. Gravitational interaction of regularized quantum vacuum energy. *Phys. Rev. D* **2014**, *89*, 064027. [CrossRef]
82. Schwinger, J. Casimir effect in source theory. *Lett. Math. Phys.* **1975**, *1*, 43–47. [CrossRef]
83. Schwinger, J. Casimir effect in source theory II. *Lett. Math. Phys.* **1992**, *24*, 59–61. [CrossRef]
84. Lima, A.P.C.M.; Alencar, G.; Landim, R.R. Null second order corrections to Casimir energy in weak gravitational field: The Schwinger's approach. *J. Cosmol. Astropart. Phys.* **2021**, *01*, 056. [CrossRef]
85. Nazari, B. Quasi-local stress–tensor formalism and the Casimir effect. *Mod. Phys. Lett. A* **2022**, *37*, 2250160. [CrossRef]
86. Sorge, F.; Wilson, J.H. Casimir effect in free fall towards a Schwarzschild black hole. *Phys. Rev. D* **2019**, *100*, 105007. [CrossRef]
87. Sorge, F. Casimir energy in Kerr spacetime. *Phys. Rev. D* **2014**, *90*, 084050. [CrossRef]
88. Ferrara, S.; Scherk, J.; Zumino, B. Algebraic properties of extended supergravity theories. *Nucl. Phys. B* **1977**, *121*, 393–402. [CrossRef]
89. Deser, S.; Zumino, B. Broken Supersymmetry and Supergravity. *Phys. Rev. Lett.* **1977**, *38*, 1433–1436. [CrossRef]
90. Lämmerzahl, C.; Dittus, H. Book Review: The Search for Non-Newtonian Gravity by E. Fischbach und C. L. Talmadge. *Gen. Rel. Grav.* **2000**, *32*, 2105–2107. [CrossRef]

91. Bordag, M.; Geyer, B.; Klimchitskaya, G.L.; Mostepanenko, V.M. New constraints for non-Newtonian gravity in the nanometer range from the improved precision measurement of the Casimir force. *Phys. Rev. D* **2000**, *62*, 011701. [CrossRef]
92. Mostepanenko, V.M.; Decca, R.S.; Fischbach, E.; Klimchitskaya, G.L.; Krause, D.E.; Lopez, D. Stronger constraints on non-Newtonian gravity from the Casimir effect. *J. Phys. A Math. Theor.* **2008**, *41*, 164054. [CrossRef]
93. Bezerra, V.B.; Klimchitskaya, G.L.; Mostepanenko, V.M.; Romero, C. Advance and prospects in constraining the Yukawa-type corrections to Newtonian gravity from the Casimir effect. *Phys. Rev. D* **2010**, *81*, 055003. [CrossRef]
94. Klimchitskaya, G.L.; Romero, C. Strengthening constraints on Yukawa-type corrections to Newtonian gravity from measuring the Casimir force between a cylinder and a plate. *Phys. Rev. D* **2010**, *82*, 115005. [CrossRef]
95. Bezerra, V.B.; Klimchitskaya, G.L.; Mostepanenko, V.M.; Romero, C. Constraints on non-Newtonian gravity from measuring the Casimir force in a configuration with nanoscale rectangular corrugations. *Phys. Rev. D* **2011**, *83*, 075004. [CrossRef]
96. Mostepanenko, V.M.; Bezerra, V.B.; Klimchitskaya, G.L.; Romero, C. New constraints on Yukawa-type interactions from the Casimir effect. *Int. J. Mod. Phys. A* **2012**, *27*, 1260015. [CrossRef]
97. Klimchitskaya, G.L.; Mohideen, U.; Mostepanenko, V.M. Constraints on non-Newtonian gravity and light elementary particles from measurements of the Casimir force by means of a dynamic atomic force microscope. *Phys. Rev. D* **2012**, *86*, 065025. [CrossRef]
98. Klimchitskaya, G.L.; Mohideen, U.; Mostepanenko, V.M. Constraints on corrections to Newtonian gravity from two recent measurements of the Casimir interaction between metallic surfaces. *Phys. Rev. D* **2013**, *87*, 125031. [CrossRef]
99. Klimchitskaya, G.L.; Kuusk, P.; Mostepanenko, V.M. Constraints on non-Newtonian gravity and axionlike particles from measuring the Casimir force in nanometer separation range. *Phys. Rev. D* **2020**, *101*, 056013. [CrossRef]
100. Khoury, J.; Weltman, A. Chameleon cosmology. *Phys. Rev. D* **2004**, *69*, 044026. [CrossRef]
101. Hinterbichler, K.; Khoury, J. Symmetron fields: Screening long-range forces through local symmetry restoration. *Phys. Rev. Lett.* **2010**, *104*, 231301. [CrossRef] [PubMed]
102. Elder, B.; Vardanyan, V.; Akrami, Y.; Brax, P.; Davis, A.C.; Decca, R.S. Classical symmetron force in Casimir experiments. *Phys. Rev. D* **2020**, *101*, 064065. [CrossRef]
103. Sedmik, R.I.P. Casimir and non-Newtonian force experiment (CANNEX): Review, status, and outlook. *Int. J. Mod. Phys. A* **2020**, *35*, 2040008. [CrossRef]
104. Klimchitskaya, G.L.; Mostepanenko, V.M.; Sedmik, R.I.P.; Abele, H. Prospects for searching thermal effects, non-Newtonian gravity and axion-like particles: Cannex test of the quantum vacuum. *Symmetry* **2019**, *11*, 407. [CrossRef]
105. Tripathy, S.K. Modelling Casimir wormholes in extended gravity. *Phys. Dark Univ.* **2021**, *31*, 100757. [CrossRef]
106. Morris, M.S.; Thorne, K.S. Wormholes in spacetime and their use for interstellar travel: A tool for teaching general relativity. *Am. J. Phys.* **1988**, *56*, 395–412. [CrossRef]
107. Pavlovic, P.; Sossich, M. Wormholes in viable $f(R)$ modified theories of gravity and eeak energy condition. *Eur. Phys. J. C* **2015**, *75*, 117. [CrossRef]
108. De Falco, V.; Battista, E.; Capozziello, S.; De Laurentis, M. Testing wormhole solutions in extended gravity through the Poynting–Robertson effect. *Phys. Rev. D* **2021**, *103*, 044007. [CrossRef]
109. De Falco, V.; Battista, E.; Capozziello, S.; De Laurentis, M. Reconstructing wormhole solutions in curvature based Extended Theories of Gravity. *Eur. Phys. J. C* **2021**, *81*, 157. [CrossRef]
110. Garattini, R. Casimir wormholes. *Eur. Phys. J. C* **2019**, *79*, 951. [CrossRef]
111. Garattini, R. Yukawa–Casimir wormholes. *Eur. Phys. J. C* **2021**, *81*, 824. [CrossRef]
112. Carvalho, I.D.D.; Alencar, G.; Muniz, C.R. Gravitational bending angle with finite distances by Casimir wormholes. *Int. J. Mod. Phys. D* **2022**, *31*, 2250011. [CrossRef]
113. Samart, D.; Tangphati, T.; Channuie, P. Charged traversable wormholes supported by Casimir energy with and without GUP corrections. *Nucl. Phys. B* **2022**, *980*, 115848. [CrossRef]
114. Avalos, R.; Fuenmayor, E.; Contreras, E. Traversable wormholes with like-Casimir complexity supported with arbitrarily small amount of exotic matter. *Eur. Phys. J. C* **2022**, *82*, 420. [CrossRef]
115. Sokoliuk, O.; Baransky, A.; Sahoo, P.K. Probing the existence of the ZTF Casimir wormholes in the framework of f(R) gravity. *Nucl. Phys. B* **2022**, *980*, 115845. [CrossRef]
116. Hassan, Z.; Ghosh, S.; Sahoo, P.K.; Bamba, K. Casimir wormholes in modified symmetric teleparallel gravity. *Eur. Phys. J. C* **2022**, *82*, 1116. [CrossRef]
117. Hassan, Z.; Ghosh, S.; Sahoo, P.K.; Rao, V.S.H. GUP corrected Casimir wormholes in $f(Q)$ gravity. *Gen. Rel. Grav.* **2023**, *55*, 90. [CrossRef]
118. de Oliveira, P.H.F.; Alencar, G.; Jardim, I.C.; Landim, R.R. On the Traversable Yukawa–Casimir wormholes. *Symmetry* **2023**, *15*, 383. [CrossRef]
119. Oliveira, P.H.F.; Alencar, G.; Jardim, I.C.; Landim, R.R. Traversable Casimir wormholes in D dimensions. *Mod. Phys. Lett. A* **2022**, *37*, 2250090. [CrossRef]
120. Alencar, G.; Bezerra, V.B.; Muniz, C.R. Casimir wormholes in $2+1$ dimensions with applications to the graphene. *Eur. Phys. J. C* **2021**, *81*, 924. [CrossRef]

121. Harko, T.; Lobo, F.S.N.; Mak, M.K. Wormhole geometries supported by quark matter at ultra-high densities. *Int. J. Mod. Phys. D* **2014**, *24*, 1550006. [CrossRef]
122. Chernodub, M.N.; Goy, V.A.; Molochkov, A.V.; Nguyen, H.H. Casimir effect in Yang–Mills theory in $D = 2 + 1$. *Phys. Rev. Lett.* **2018**, *121*, 191601. [CrossRef]